ACS APPLIED NANO MATERIALS
Cite This: ACS Appl. Nano Mater. 2019, 2, 7103−7113
Article
www.acsanm.org

Computational Study of the Effect of Functional Groups on Water Adsorption in Mesoporous Carbons: Implications for Gas Adsorption

Xuan Peng,*[,†] Jose Manuel Vicent-Luna,[‡] Surendra Kumar Jain,[§] Qibing Jin,[†] and Jayant Kumar Singh[§]

[†]College of Information Science and Technology, Beijing University of Chemical Technology, Beijing 100029, PR China
[‡]Department of Physical, Chemical and Natural Systems, Universidad Pablo de Olavide, Ctra. Utrera Km 1, ES-41013 Seville, Spain
[§]Department of Chemical Engineering, Indian Institute of Technology Kanpur, Kanpur 208016, India

Supporting Information

ABSTRACT: The adsorption and diffusion of water in realistic CMK-1, CMK-3, and CMK-5 carbon models at 300 K has been studied via grand canonical Monte Carlo and molecular dynamics simulations. The presence of −COOH and −OH functional groups has been found to be crucial to describe the adsorption process, while the models without functional groups are unable to capture the host−guest interactions. Functional groups were attached in cylindrical shells on the outer walls of CMK models in 2 and 4 cylindrical shells to study the effect of their concentration and location on water adsorption. The adsorption isotherm starts at a lower chemical potential, with water adsorbed near functional groups forming small clusters. On increasing chemical potential the water cluster grows and merges to form bigger clusters and completely fills the pores. We also analyzed the isosteric heat, radial distribution functions, hydrogen bond, and cluster size of water molecules. It indicates that the adsorption occurs due to the formation and growth of water clusters. For CMK-1, CMK-3, and CMK-5 models with functional groups, the pore filling happens at lower chemical potential, when compared to the models without functional groups, owing to the presence of active sites which favors the nucleation of water molecules. The effect of functional groups is also remarkable in the diffusion of water inside the pores of CMK-1, CMK-3, and CMK-5 models, lowering the mobility of the adsorbed molecules. The agreement between the results of the models with functional groups and the experimental observations makes the presence of these groups necessary to study the adsorption and diffusion of water in CMK-1, CMK-3, and CMK-5 carbon models.

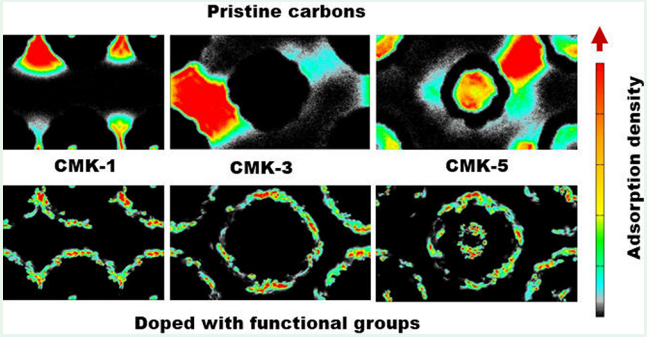

KEYWORDS: *mesoporous carbons, adsorption, diffusion, water, functional groups, molecular simulation*

1. INTRODUCTION

The structure and thermodynamic and dynamic properties of simple fluids in nanoporous carbons have been investigated exhaustively.[1,2] However, water adsorption inside hydrophobic carbon materials is still challenging. Water adsorption in hydrophobic nanopores typically exhibits a complete pore filling by a capillary-condensation mechanism, where a steeped isotherm appears after a relatively high pressure. It also shows a large adsorption/desorption hysteresis loops.[3] There are a number of studies of the water adsorption on carbon surfaces or in porous carbons using molecular simulations,[4,5,14−16,6−13] but there is a lack of investigations on water adsorption in carbon mesopores. Water adsorption has also been proposed as a characterizing technique in measuring the amount of oxygenated functional groups present on the surface of porous carbons.[17−19]

It is also well-known that the design and development of water stable porous nanomaterials is critical for certain industrial applications such as gas storage, separation, and catalysis.[20,21] Of particular importance for energetic and environmental applications, water adsorption is often detrimental for methane storage and carbon dioxide capture using hydrophilic materials since water acts as a strong competitor. Nevertheless, it was demonstrated that controlled water adsorption can enhance methane storage in activated carbons[22] and carbon dioxide capture in metal organic frameworks (MOFs).[23]

Water adsorption in carbons is known to be strongly affected by the presence and density of oxygenated groups on the carbon surface.[24−27] Striolo et al.[8] studied the effect of carbonyl groups attached to the carbon nanotubes. The carbonyl groups were concentrated in a narrow section along the carbon nanotube. Their study showed that the presence of carbonyl groups lowers the pore filling pressure, lowers the

Received: August 26, 2019
Accepted: October 17, 2019
Published: October 17, 2019

DOI: 10.1021/acsanm.9b01633
ACS Appl. Nano Mater. 2019, 2, 7103−7113

capillary condensation pressure, and also reduces the width of the adsorption/desorption hysteresis loops with respect to those in bare carbon nanotubes. Their results further indicated that at low pressures a small cluster of hydrogen-bonded water molecules is formed near the carbonyl groups. As the pressure increases, the cluster grows until the pore is completely filled with water molecules.

Do and co-workers[28] studied the water adsorption in finite sized slit pores in the presence of hydroxyl groups. Two different locations of the functional group, either at the center or at the corner of the upper pore wall, were used to study the effects of the position and the concentration of the functional group on the adsorption isotherm. Their findings can be summarized in the following points. (a) The adsorption phenomena started early due to the favorable adsorption of water molecules around functional groups via hydrogen bonding. (b) The isotherms for models with functional groups was higher than those of pristine models. (c) The relative pressure at which pore filling occurs was lower for the models with functional groups and was below the saturation pressure for models with functional groups. This finding was consistent with what has been observed in experiments.[29−32] This is due to the greater interaction energy between water molecules and functional groups, and that leads to favorable nucleation of water clusters. (d) The hysteresis loop was smaller for models with functional groups as opposed to pristine models.

The authors also reported the effects of the position of functional groups on adsorption. They found that the adsorption isotherm for the center topology model is greater than that for the corner topology model at low relative pressures. The effect of location of active sites on the adsorption of water is also observed in the literature.[33,34] The authors also studied the effect of the concentration of functional groups on adsorption. Their findings can be summarized as follows: (a) In the low pressure regime, the amount of water adsorbed increases with increase in the concentration of functional groups. This is due to the presence of more active adsorption sites for water to interact with. Their simulation results agree with the experimental observations of Morimoto and Miura,[35−38] which showed that a reduction in the amount of functional groups resulted in a drastic decrease in water adsorption. (b) An increase in concentration of functional groups leads to marginally early onset of pore filling. This could be because the pore filling is governed mainly by the water−water interaction. It has been found that adsorption of water is appreciable at low pressures, and pore filling occurs at lower pressures. At low pressures, isolated water molecules bond to oxygenated surface sites, but this stage is quickly followed by the buildup of water clusters around those sites. Where possible, water molecules seek locations where they can form multiple H-bonds on adsorption, by bonding either to several preadsorbed water molecules or to a water molecule and a surface site.[25]

In a recent work, Sarkisov et al.[39] studied water adsorption in a high surface area activated carbon with carboxylate functional groups. Their model was able to reproduce reasonably well the shape of the adsorption and scanning desorption isotherms. However, the model the authors considered contained only micropores and did not have mesopores. So, it will be interesting to compare the results obtained by the authors with the carbon models containing mesopores.

In this work, we have carried out molecular simulations to study the adsorption of water in several mesoporous carbons, namely, CMK-1, CMK-3, and CMK-5. The aim of this study is to understand in depth the mechanisms that govern the adsorption of water in these hydrophobic materials. Thommes et al.[40] investigated water adsorption in CMK-1 and CMK-3, among other mesoporous carbons, and showed the potential of this fluid for the physical adsorption characterization of porous solids as a probe molecule. They suggested that the water adsorption in hydrophobic mesoporous carbons slightly deviates from the usual capillary condensation, but it is consistent with the pore filling of a clustering mechanism. Weinberger et al.[41] carried out water vapor adsorption experiments in CMK-5 carbon. They performed an oxidative treatment with acidic perfsulfate solution to chemically modify the original material. This modification allows the creation of oxygen-containing functionalities at the pore walls of the carbon which affects the adsorption of water. Further investigations are needed to understand the mechanisms that govern the water adsorption in these mesoporous materials.

Recently, we have developed realistic molecular models for CMK-1, CMK-3, and CMK-5 carbons.[42] Furthermore, we studied the adsorption of water in pristine CMK-3 and CMK-5 models, without any attached functional groups.[43] It was found that the water adsorption was negligible at low pressure with sudden pore filling at higher pressures. The representative snapshots at different pressures showed water clusters form, and they grow in size as pressure increases, which results in pore filling. This is contrary to water adsorption in microporous carbons, such as saccharose-based activated carbon (CS400, CS1000, and CS1000a) molecular models developed by hybrid reverse Monte Carlo (HRMC).[44] The pore size of CS400 and CS1000 is about 5 Å, which is too narrow to allow the nucleation of water molecules. CS1000a shows a pore size of about 10 Å in a pore network in which water molecules can form large clusters. However, this pore size is much smaller than those shown in mesoporous carbons, such as CMK-1, CMK-3, and CMK-5. These structures have pore sizes of about 30−40 Å, which were modeled in our calculations with a pore size larger than 20 Å of diameter. The difference between the pores of the microporous activated carbons and the mesoporous carbons is crucial for the adsorption of water because the critical diameter for water adsorption is about 20 Å of diameter. In pores with sizes below this value, water adsorption is driven by the direct interaction with the internal surface of the adsorbent and followed by the cluster formation. On the contrary, in pores large than the critical diameter the adsorption is due to capillary condensation preceded by cluster adsorption. In our previous study of water adsorption on CMK-3 and CMK-5,[43] the nucleation of water in the most hydrophobic structures, i.e., without functional groups, was investigated. The adsorption isotherm showed a steeped behavior from nonadsorption to almost saturation without intermediate steeps. That study described the behavior of water molecules when adsorbed in hydrophobic materials with large pores. However, it fails to describe properly the adsorbate−adsorbent interactions. This led us to investigate in detail in the present work the role of the adsorbate/adsorbent in a more realistic material. Apart from the nucleation of water molecules, we describe the diffusion of guest molecules in pores with and without functional groups. Moreover, we compare the adsorption energies with the experimental measurements. We highlight the importance of

DOI: 10.1021/acsanm.9b01633
ACS Appl. Nano Mater. 2019, 2, 7103−7113

the addition of functional groups to describe completely the adsorption and diffusion behavior of water in hydrophobic carbon materials with large pores.

In this work, we attach oxygen containing functional groups (−COOH and −OH) to the CMK-1, CMK-3, and CMK-5 pore surfaces and study the influence of these functional groups on the adsorption of water. We compare the results obtained with the models with and without functional groups. We chose to use −COOH and −OH functional groups as these functional groups are believed to be predominant in porous carbons and have been used by different researchers in molecular simulation studies of water in porous carbons. We also study the effect of the concentration and location of the functional groups[6,11] attached to CMK models on water adsorption. The separate study of the effect of OH and COOH functional groups in water adsorption on carbonaceous systems has been already studied. Moulin et al.[45] found that OH functional groups have insignificant effect on water adsorption when compared with the effect of COOH functional groups. This is because the presence of carbonyl and carboxyl groups strongly increases the polarity of the adsorbents; hence, the pore surface becomes more hydrophilic. In this work, we choose the model including both functional groups, since it emulates the most realistic conditions,[41] and compare them with the structures without functional groups. The aim of this work is to investigate in detail how the addition of functional groups affects the adsorption and diffusion behavior and also the structure of adsorbed water in CMK-1, CMK-3, and CMK-5 mesoporous carbon models. In addition to adsorption isotherms, we also present isosteric heat of adsorption, which can be compared with the experimental observations, ensuring the validity of the models used in this work. We describe the structure of confined water, via radial distribution functions, hydrogen bonds, and cluster analysis. Finally, we analyze the effect of the functional groups in CMK models in the diffusion of adsorbed water and in the activation energy of the diffusion process.

2. SIMULATION METHODOLOGY

2.1. CMK-1, CMK-3, and CMK-5 Models. The structural model of CMK used here comes from our previous research work.[42] By performing the GCMC simulation of the carbon source adsorption in the cylindrical pore of MCM-41 zeolite, we can obtain the structures of carbon rods and carbon pipes under certain thermodynamic conditions. The carbon rods are further arranged in cubic and hexagonal lattices to create molecular models for CMK-1 and CMK-3, respectively. Similarly, the carbon pipes were decorated in a hexagonal lattice to obtain molecular models for CMK-5. In addition, we added random interconnections between carbon rods and between carbon pipes in the CMK models to mimic the experiments that the carbon rods and carbon pipes in CMK-3 and CMK-5 materials are connected via small interconnections.

We added different functional groups to the CMK-1, CMK-3, and CMK-5 models to study the effect of functional groups on water adsorption. The method of adding functional groups to the CMK model is similar to our previous works on the HRMC model.[44,46] The general rule is that the atoms on the functional groups grow at a certain bond length and bond angle and ensure that they do not overlap with atoms on the carbon model and other functional groups. For CMK-5, functional groups can be grown both inside and outside the tube. In this work, two different groups are used, namely, carboxyl (−COOH) and hydroxyl (−OH) groups. The functional groups are added in a cylindrical shell on the walls of the CMK-1, CMK-3, and CMK-5 models. To study the effect of concentration and localization of functional groups on water adsorption, we added functional groups in 2 cylindrical shells and 4 cylindrical shells on the walls of CMK-1, CMK-3, and CMK-5 models. For CMK-5 models, functional groups were added in the cylindrical shells of the inner wall and outer wall, respectively. The distances, angles, and potential parameters[10] are tabulated in Table S1 (see Supporting Information). The number of −OH groups and −COOH groups attached to the CMK-1, CMK-3, and CMK-5 models are shown in Table 1. We show snapshots of the CMK-1, CMK-3, and CMK-5 models with attached functional groups in Figure 1.

Table 1. Number of Functional Groups Present in Different CMK Models

CMK model	no. of carbon atoms	no. of −COOH groups	no. of −OH groups
CMK-1 2 shells	13006	256	172
CMK-1 4 shells	12784	418	232
CMK-3 2 shells	14364	246	161
CMK-3 4 shells	14158	361	252
CMK-5 2 shells	7793	305	173
CMK-5 4 shells	7622	443	206

2.2. Grand Canonical Monte Carlo (GCMC) Simulation. We use the standard GCMC algorithm to calculate the adsorption equilibria of water in the CMK models, where four types of particle moves including translation, rotation, insertion, and deletion are attempted to ensure the chemical potential of the pore phase equal to that of the bulk phase. In the simulations, periodic boundary conditions are imposed on *xyz* directions. For each state, we generated 2×10^9 water configurations and discarded the first 40% of the moves to guarantee equilibrium. The remaining states were divided into 20 blocks for a ensemble average. The TIP4P model was used to describe the water molecule,[43,47] and the potential parameter for the carbon atoms in the CMK matrix was taken from our previous publication.[43] The cutoff radius is set to 12 Å for the LJ and electrostatic potentials, and the Lorentz−Berthelot mixing rule was used to obtain cross interaction potential parameters.

2.3. Molecular Dynamics Simulation. To study the dynamical properties of water in the mesoporous carbons models and the effect of the functional groups, we carried out molecular dynamics (MD) simulations in the NVT ensemble at different temperatures. We study the dynamics of water molecules in the low coverage regime in the CMK-1, CMK-3, and CMK-5 models with and without functional groups in a temperature range between 283 and 328 K. To do so, we load each structure with 100 water molecules to ensure a good statistical average. We run a total of 2×10^7 cycles with a time step of 0.001 ps after a short equilibration of 2×10^5 cycles to relax the systems in their equilibrium energy. The trajectories were recorded every 5 ps during the 20 ns of simulation time for the production runs. From this trajectory we computed the self-diffusion coefficients using the Einstein relation in the diffusive regime of the mean squared displacement as a function of the time plot.

2.4. Structural Properties of Confined Water. To investigate the structure of adsorbed water, we calculated the radial distribution function between the oxygen atoms of water molecules goo(r), the radial distribution function between the oxygen and the hydrogen atoms goh(r), and the hydrogen bond statistics from geometrical criteria.[48] Using a depth first search algorithm, we also calculated the water cluster size from the hydrogen bond information. More details for the algorithms can be found in our previous work.[43]

DOI: 10.1021/acsanm.9b01633
ACS Appl. Nano Mater. 2019, 2, 7103−7113

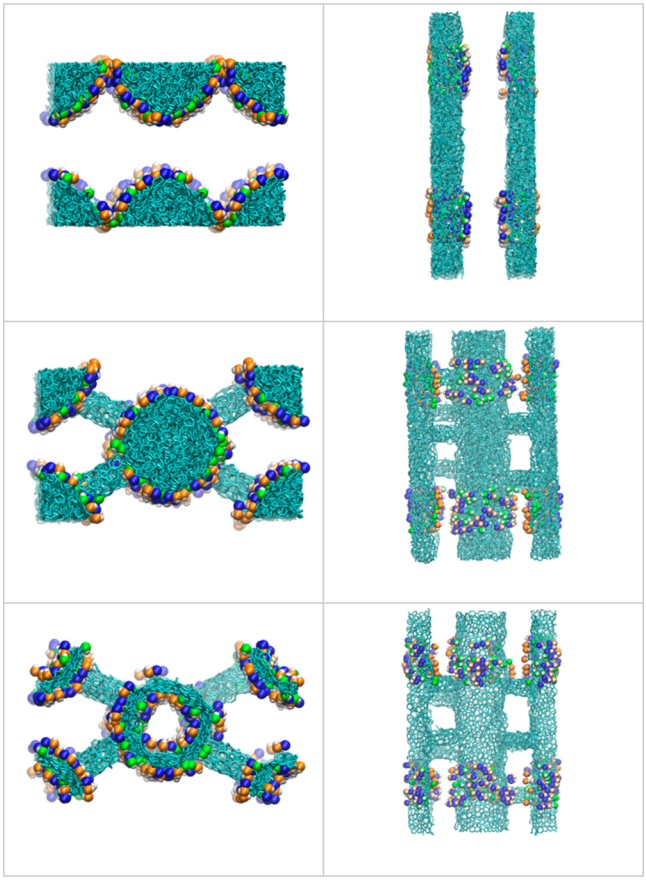

Figure 1. Front view and side view of (top) CMK-1, (middle) CMK-3, and (bottom) CMK-5 models. The functional groups are concentrated in 2 cylindrical shells. Similarly, we have added 4 cylindrical shells to the CMK-1, CMK-3, and CMK-5 models (not shown here). Color code: blue and orange reflects oxygen atoms of the −COOH group. Green reflects oxygen atoms of the −OH group, and white reflects hydrogen atoms of both the −COOH and −OH groups.

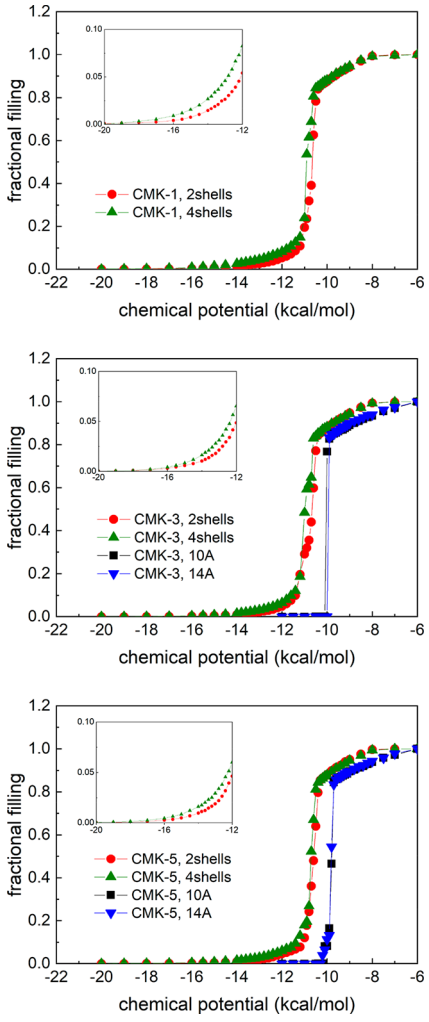

Figure 2. Water adsorption isotherms in CMK-1, CMK-3, and CMK-5 models with functional groups and without functional groups.

3. RESULTS AND DISCUSSION

3.1. Pore Size Distribution (PSD) of the CMK Models. We used the method of Bhattacharya et al.[49] to calculate the pore size distribution of the CMK models. Figure S1 shows the pore size distribution of the CMK-1, CMK-3, and CMK-5 models (see Supporting Information). From the figure, it can be seen that the CMK-1 model has a peak around 13 Å, which is the distance between carbon rods at the opposite end of the slit shaped pore. CMK-3 has a somewhat wide pore size distribution, which shows that we cannot use cylindrical pores to describe the pores of the CMK-3 materials. Since the carbon rods in the CMK-3 models are present in a hexagonal lattice, there is a wide pore size distribution. CMK-5 models also have a wide pore size distribution, and this is also due to the carbon pipes arranged in hexagonal lattice. There is a peak at around 9 Å in the PSD of CMK-5, which is due to the inner porosity of the carbon pipes.

3.2. Adsorption Isotherms of Water in CMK Models. In Figure 2, we present the adsorption isotherms of water in CMK models with two and four cylindrical shells of functional groups. To highlight the effect of the addition of these functional groups, we included the adsorption isotherms of water in CMK-3 and CMK-5 with two pore sizes and without functional groups taken from our previous work.[43] Desorption isotherms were not computed due to the high computational cost that is entailed to reach equilibrium in simulations of water nucleation in large pore-based materials. In this context, we are more interested in the adsorption phenomena of water and especially what occurs when the first molecules of water are in contact with the pore walls. We observe that the models containing functional groups show more distinct behavior for water adsorption than the pristine models. On the one hand, the presence of functional groups reduces the chemical potential where the water molecules start adsorbing. This is due to the presence of −COOH and −OH functional groups that provide active sites for water adsorption. As can be seen in the inset figures, the adsorption starts at lower chemical potential when increasing the concentration of functional groups. On the other hand, in the models without functional groups, the adsorption isotherms show a sudden increase at certain chemical potential, while in the models with functional groups we can see a soft start of the adsorption isotherm. This is due to the adsorption in the functional groups, before the nucleation of the water molecules. In the models without functional groups, the adsorption behavior is governed only by the nucleation of water molecules. These findings are in concordance with the clustering mechanism suggested by Thommes et al.[40] for water adsorption in CMK-1 and CMK-3. However, the presence of functional groups not only provides

DOI: 10.1021/acsanm.9b01633
ACS Appl. Nano Mater. 2019, 2, 7103−7113

active sites for adsorption but also facilitates the nucleation process. The shape of the adsorption isotherms of water in the CMK models with functional groups is in good agreement with the experimental results for these adsorbents. Figure S2 shows the experimental adsorption isotherms in CMK-1 and CMK-3 reported by Thommes et al.[40] and in CMK-5 reported by Weinberger et al.[41] Figure S2 (top) represents the adsorption isotherms in terms of fractional filling, while the Figure S2 (bottom) shows the gravimetric loading in mg/g to highlight the differences between the three materials. Due to the differences between the size of the real structures and the models used in this work, we cannot make a direct comparison of the adsorption isotherms. A more direct comparison can be done for the energies of adsorption that will be discussed in the following sections. However, there are some similarities between the simulations and the experimental results, which make realistic the CMK models used in this work. Apart from the smooth start in the adsorption isotherms, we can see in Figure S2 that the water adsorption occurs at the same partial pressure for the three CMK models, while the simulated results of Figure 2 indicates that the water adsorption takes place at the same chemical potential. On the one hand, the models without functional groups provide an approximate idea about the adsorption mechanism in the CMK-1, CMK-3, and CMK-5 models. On the other hand, the agreement in the shape of the computed adsorption isotherms in the CMK models with functional groups and the experimental values indicates that the addition of these functional groups is necessary for a correct description of the process.

3.3. Configuration of Confined Water in the Pores of the CMK Models. Figure 3 and Figures S3−S6 illustrate the snapshots of the pore filling of CMK models. It can be seen clearly from the snapshots that water adsorption occurs around functional groups at low chemical potential, where they act as nucleation sites for other water molecules to adsorb by forming hydrogen bonds. Our results show a formation of small water clusters around the functional groups, and the water clusters grow with increasing chemical potential and merge to form bigger water clusters to completely fill the pores. This mechanism differs from that obtained for the CMK-3 and CMK-5 models without functional groups.[43] In CMK-3 without functional groups the pores are filled drastically, while in CMK-5 without functional groups the pore filling occurs in two steps. First water molecules completely fill the inner porosity and then water starts adsorbing in the outer porosity. In this case, the three CMK models with functional groups show a similar pore filling mechanism, where it occurs at lower chemical potential for models with 4 cylindrical shells compared with those with 2 cylindrical shells. Once the nucleation starts around the functional groups, water clusters form bridges between two carbon rods in CMK-1 and CMK-3 before the complete pore filling. In the case of CMK-5 models, the water clusters form bridges between the radially opposite sides of functional groups present in inner and outer porosity. The inner pores of the CMK-5 models are filled first due to the smaller size of these cavities.

3.4. Isosteric Heat of Adsorption. In order to investigate the accuracy of the CMK models used in this work to describe the adsorption of water, we investigate the energetic interactions involved in the process. Figure 4 shows the comparison of the computed and experimental isosteric heats of adsorption of water in CMK-1, CMK-3, and CMK-5 models. We included the isosteric heat of adsorption predicted

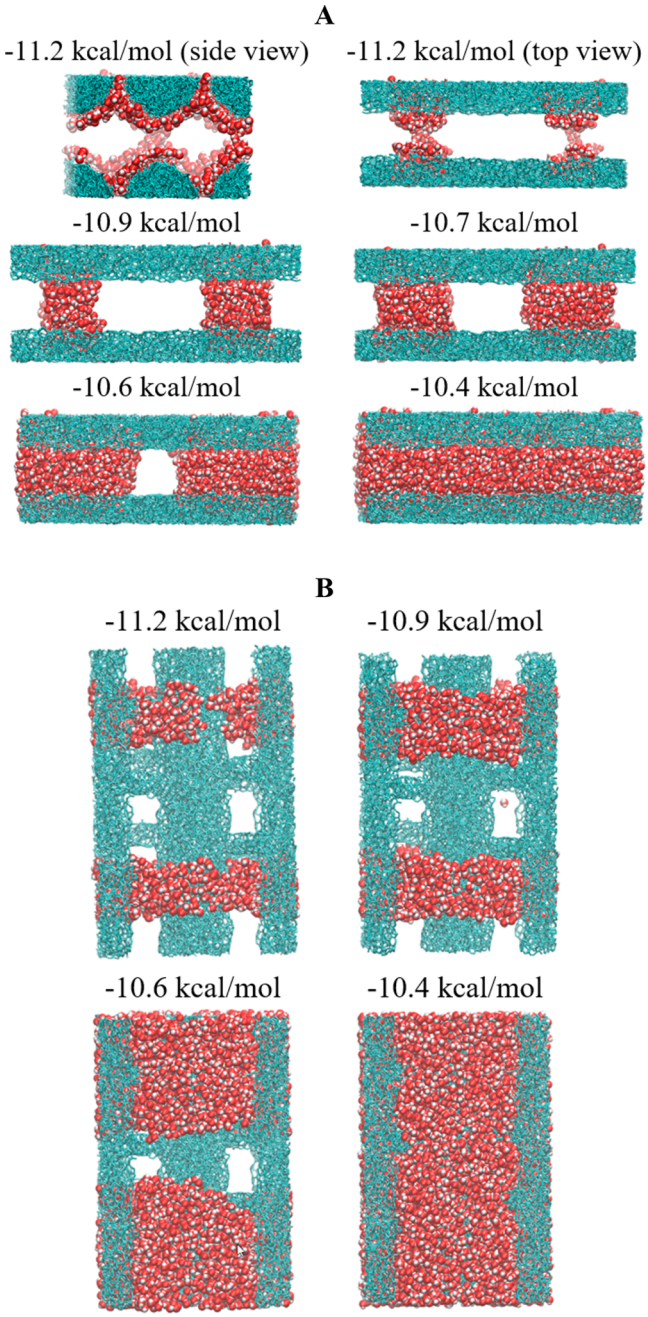

Figure 3. Snapshot of water adsorption in CMK models with functional groups in 2 cylindrical shells, (a) CMK-1 and (b) CMK-3

from the experimental isotherms[40,41] (see Figure S2) by using the Dubinin−Polanyi theory.[50] With this theory, one can reduce the two-dimensional description of the adsorption equilibrium of a water/adsorbent pair (P, T) to the temperature independent characteristic curve. The characteristic curve is a relation of the adsorption potential as a function of the adsorbed specific volume.[51] Then, the isosteric heat of adsorption can be calculated as the heat released during the adsorption process concerning the enthalpy of evaporation, the adsorption potential, and an entropic term related to the slope of the characteristic curve.[51]

In Figure 4, there is good agreement between the computed isosteric heats of adsorption and experimental observations when the models with functional groups are used. However,

DOI: 10.1021/acsanm.9b01633
ACS Appl. Nano Mater. 2019, 2, 7103−7113

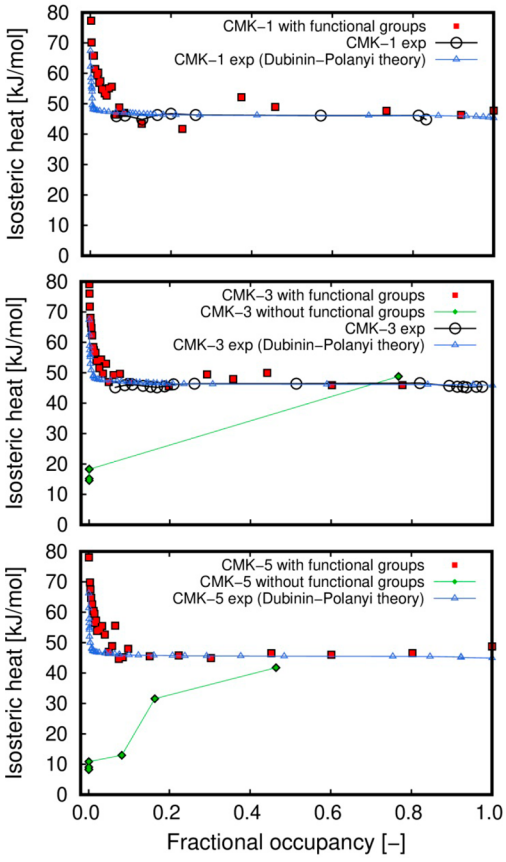

Figure 4. Isosteric heats of adsorption of water in CMK-1, CMK-3, and CMK-5 models as a function of the fractional occupancy. Experimental values were taken from references 40 and 41.

the models which do not contain functional groups fail to describe the host–guest interactions, especially at very low coverage. The results predicted by the Dubinin–Polanyi theory and the computed heats in this work show a high interaction between the adsorbents and water molecules at very low loading. In this region, the isosteric heat values are very high (~80 kJ/mol). This is due to the interaction of the first adsorbed water molecules with the –OH and –COOH groups of the structures. Models without the functional groups are extremely hydrophobic and predict a very low host–guest interaction. This interaction of the water molecules with the functional groups allows for the nucleation of the molecules via hydrogen bonds as described before. Once the nucleation starts, the isosteric heats converge to an almost constant value in a wide range of loadings and independently of the structure. This value is about 45 kJ/mol which corresponds with the condensation enthalpy of bulk water. This means that the adsorbed water behaves like it is in the liquid phase when it is confined in the pores. This fact confirms the validity of the CMK models used here to analyze the molecular mechanisms that take place during the water vapor adsorption process. Figure 4 does not contain error bars; however, the agreement with the experiments gives confidence to the computed results. Error bars of the heat of adsorption, especially at high coverage, are difficult to estimate, due to the clustering of water molecules making the insertion/deletion of molecules in the MC scheme difficult. This fact cannot be solved even with much longer simulations. However, we provided the average number of adsorbed molecules and the corresponding energy at a chemical potential of −11 kcal/mol in Table S2. The table also contains their error values, which suggest that the fluctuations of the heat of adsorption are in an acceptable range.

To gain insights into the origin of the behavior of the isosteric heat of adsorption in CMK models with functional groups, we computed the fluid–fluid and the fluid–wall contributions which are shown in Figure 5. Here, the fluid–

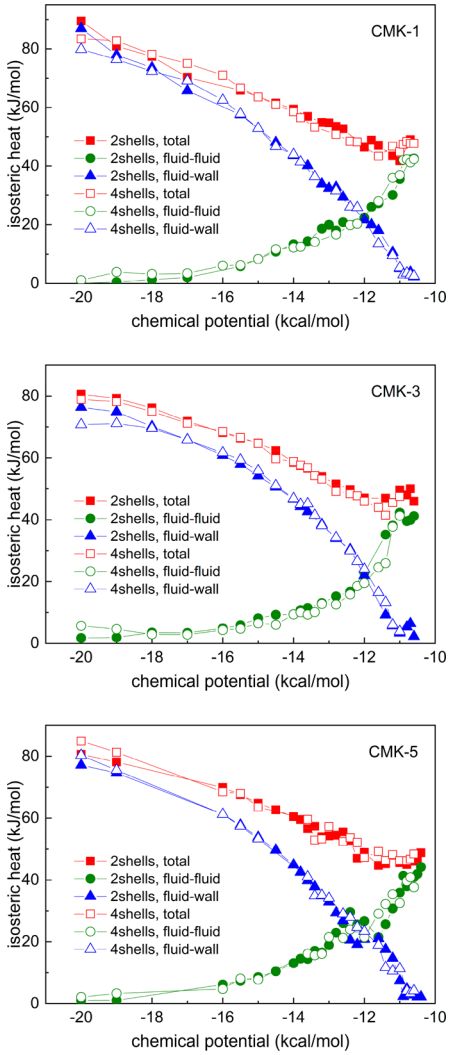

Figure 5. Isosteric heats of water adsorption in CMK-1, CMK-3, and CMK-5 models contributed by fluid–fluid and fluid–wall interactions.

wall contributions are more important at low chemical potentials (owing to the presence of functional groups in the internal surface of carbon walls). Increasing the chemical potential, the active sites of functional groups are saturated, and further water adsorption occurs due to the hydrogen bonding with already adsorbed water molecules, thus decreasing the fluid–wall interactions. For the same reason, fluid–fluid interactions are negligible at very low chemical potentials; i.e., water molecules only interact with the functional groups. Increasing the chemical potential, fluid–fluid interactions gain importance reaching the value of the condensation enthalpy of bulk water (~45 kJ/mol) at the chemical potential when the pore filling occurs. The fluid–

DOI: 10.1021/acsanm.9b01633
ACS Appl. Nano Mater. 2019, 2, 7103–7113

fluid interactions of water in the CMK-3 and CMK-5 models without functional groups are very similar to those for the models with functional groups.[43] This is because the pore filling also occurs through hydrogen bonds. However, the fluid−wall interactions are lower than 10 kJ/mol in the entire range of chemical potentials. This means that the models without functional groups are extremely hydrophobic and they are not able to describe properly the host−guest interactions.

3.5. Structure of Confined Water and Hydrogen Bond Statistics. We calculated the O−O and the O−H distances corresponding to the first two coordination shells.[43,44] Tables S3−S10 show these distances for three chemical potentials. We can see that, when the chemical potential increases, the O−O and O−H distance decreases. Particularly, a greater decrease of the O−O minimum distance for the first and second hydrogen bond shell is observed due to the increase of water density. The same trend can be seen for the O−H distance, but to a lesser extent.

The structure of adsorbed water molecules is described by the g(r) for O−O and O−H atoms in the CMK models with functional groups in Figures S7−S9. In the case of the g(r) for O−O, we can see that there is a peak at ∼3 Å for all three chemical potential values. However, the height of the peak decreases with increasing chemical potential. This is not surprising since, at low chemical potential, there are fewer water molecules, and these are located a small distance from each other, which is consistent with the start of the nucleation process. In addition, a shoulder about 4 Å is shown at low chemical potentials, and the corresponding height decreases up to a small minimum at the chemical potential μ = −8.0 kcal/mol. Moreover, a small peak appears at ∼6 Å for chemical potential μ = −8.0 kcal/mol, which is absent at lower chemical potentials, demonstrating that the structure of water is more ordered at high chemical potentials. The g(r) for O−H shows similar shapes for all three chemical potentials. We see two peaks at 2 Å and 3.5 Å. Again, the height of the peak decreases with increasing chemical potential.

We present hydrogen bond statistics for the CMK models with functional groups in Figure 6. For comparison, the figure also contains the hydrogen bond statistics for bulk water at 1 atm. At low chemical potential the fractions of water molecules with 1, 2, and 3 hydrogen bonds dominate in all the cases. This means that there are no clusters with the typical tetrahedral conformation of water molecules. On increasing chemical potential, the fraction of water molecules with 3 and 4 hydrogen bonds dominate in the structure of confined water. In general, the number of water molecules having 3, 4, and 5 hydrogen bonds is larger in the pore as compared to the bulk. This suggests that the confinement facilitates the hydrogen bond formation of water molecules as compared to bulk water. This is due to the confinement into hydrophobic walls which causes a repulsion of the water molecules closer to the pore surface. Then, water molecules correlate strongly between them. It is worth mentioning that the confinement of water in CMK-5 differs slightly from the inner and outer porosity. The hydrogen bond statistics for water confined in the outer porosity of CMK-5 with functional groups is similar that for CMK-1 and CMK-3 models. However, in the inner porosity, we see a decrease of the fraction of water molecules having 3 and 4 hydrogen bonds compared with the molecules in the outer porosity. Specially, there is a reduction of the fraction of molecules forming 4 hydrogen bonds with respect to the bulk, which means a loss of the tetrahedral structure of water. This is

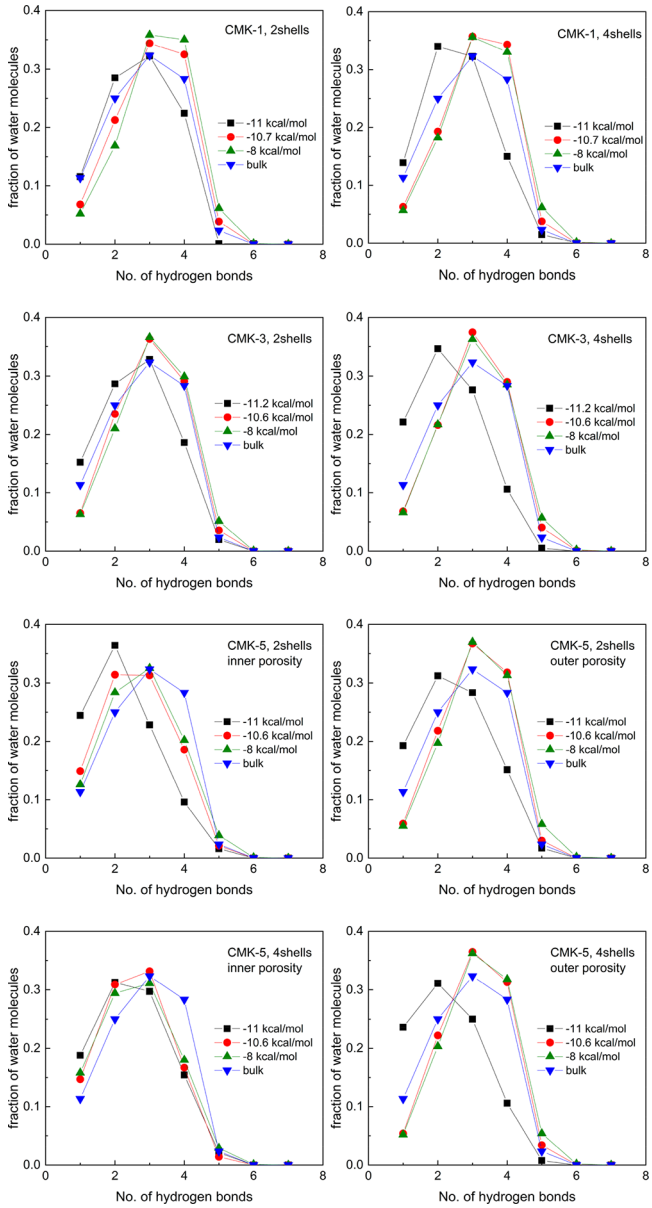

Figure 6. Hydrogen bond statistics for CMK-1, CMK-3, and CMK-5 models.

expected as the strong confinement of water molecules in the inside porosity prohibits them from forming 3-dimensional water clusters.

We calculated the clusters containing different amounts of water molecules (see the Simulation Methodology section for more information about the cluster calculation). Table 2 and

Table 2. Cluster Statistics for the CMK-1 Model (2 Shells and 4 Shells)

CMK-1	μ (kcal/mol)	size of #1 cluster	size of #2 cluster	size of #3 cluster
2 shells	−11.0	274	186	67
	−10.7	963	828	42
	−8.0	5291	13	11
4 shells	−11.0	232	111	86
	−10.7	3244	30	15
	−8.0	5092	12	11

DOI: 10.1021/acsanm.9b01633
ACS Appl. Nano Mater. 2019, 2, 7103−7113

Tables S11−S13 show the cluster statistics for the CMK models with functional groups. In general, we can see that in all the structures containing 2 and 4 shells there are 2 large water clusters at the lowest chemical potential (∼−11.0 kcal/mol). At the intermediate chemical potential (∼−10.6 kcal/mol), we see an increase of the size of the 2 water clusters in the structures with 2 cylindrical shells. However, at the same chemical potential we only see one large cluster in the CMK models with 4 cylindrical shells. This is due to the fact that the neighboring water clusters, at 4 different cylindrical shells, merge together to make one large water cluster. This is also confirmed in the snapshots. Increasing the chemical potential (−8.0 kcal/mol), we only observe one large cluster completely filling the pores of CMK-1, CMK-3, and the outer porosity of CMK-5 models. However, we see three different clusters of similar size in the inner porosity. We think this is due to the pore undulation present in the inner porosity that separates water clusters.

3.6. Self-Diffusion Coefficients and Activation Energies. We studied the dynamical properties of the confined water in the CMK models. We choose to compare the effect of the functional groups (models with 2 cylindrical shells) in the mobility of the water molecules in the low coverage regime since the adsorption isotherms and energies of adsorption show the largest differences. We fixed a loading between 1% and 2% of the total occupancy, i.e., before the drastic steep of the adsorption isotherm. In this regime, the host−guest interactions are crucial to describe properly the adsorption process. Figure 7 shows the Arrhenius plot of the natural logarithm of the self-diffusion coefficients vs the inverse of the temperature. The figure also shows the activation energies obtained from the slope of the Arrhenius plot of water in the CMK-1, CMK-3 and CMK-5 models with and without functional groups. Figure S10 depicts the temperature dependence on the self-diffusion coefficients of water at low coverage in CMK models. We observe that the presence of the functional groups lowers the self-diffusion coefficients almost two magnitude orders, which is in concordance with the strong interaction mentioned in the energetic analysis. The temperature dependence of the self-diffusion coefficients follows the Arrhenius law, which allows calculating the activation energy of the dynamic process. Figure 7 (bottom) indicates that CMK-1 and CMK-3 models without functional groups exhibit larger activation energies compared with the models with functional groups. This is due to the fact that, at low coverage, the interaction between water molecules is more important than the interaction with the structure in the models without functional groups. Thus, the water molecules start to form clusters at low coverage. This early nucleation increases the barrier energy for the diffusion process. On the contrary, in models with functional groups, water molecules are attracted by these groups which limit the diffusion of water but decrease the activation energy. However, the activation energy of water in CMK-5 is similar for the models with and without functional groups and similar to the values for the CMK-1 and CMK-3 models without functional groups. This can be due to the presence of two independent cavities formed by the inner and the outer porosity of the CMK-5 model.

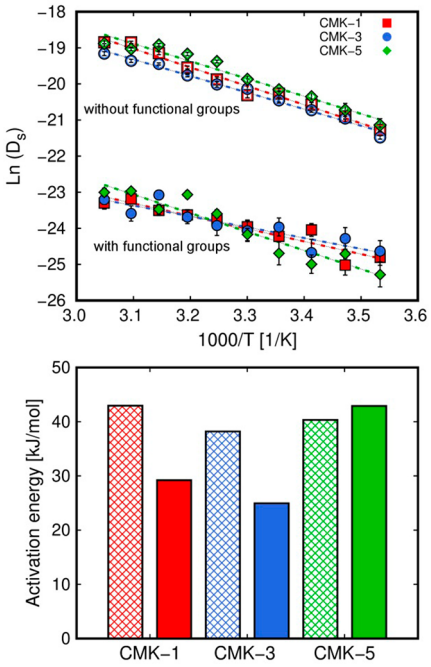

Figure 7. Arrhenius plot of the logarithm of the self-diffusion coefficients as a function of the inverse of the temperature (top) and activation energies of CMK-1, CMK-3, and CMK-5 models (bottom)

3.7. Average Occupation Profiles (AvOPs). We analyzed the effect of the functional groups in the microscopic organization of water inside the pores in the dynamic process at low coverage. Figure 8 shows the average occupation profiles of water in all models with and without functional groups. The average occupation profiles represent the most probable positions in which water molecules will be found within the cavities of the structures. The representation of the profiles is the projection over a given plane of the atomic coordinates of the water molecules. The positions of the atoms were recorded during the whole MD simulation and averaged over 4×10^3 configurations. The figure shows how, in the models without functional groups, water molecules move like clusters around the pores. However, in CMK models with functional groups, water molecules locate in the contact surface which contains the −OH and the −COOH groups. The functional groups are attached horizontally in the side ZX view (see Figure 1). The movement of water molecules is restricted to the area closed to these functional groups in the three carbon models. However, in the models without functional groups, water molecules diffuse through the cores of the channels.

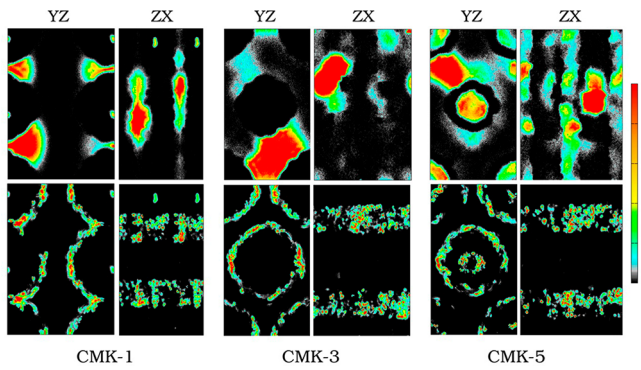

Figure 8. Average occupation profiles of water in CMK-1, CMK-3, and CMK-5 models without functional groups (top) and with functional groups (bottom) from MD simulations at low coverage.

DOI: 10.1021/acsanm.9b01633
ACS Appl. Nano Mater. 2019, 2, 7103−7113

4. CONCLUSIONS

We conducted Grand canonical Monte Carlo and molecular dynamics simulations to study the water adsorption and diffusion in realistic CMK-1, CMK-3, and CMK-5 carbon models. The effect of the attached functional groups in the pore walls on the adsorption and diffusion of water has been analyzed. The −COOH and −OH functional groups were attached in cylindrical shells in the pore walls of the three CMK models. For the CMK-5 models, there are two types of porosities: inner (intra tube) and outer (inter tube). Functional groups were attached to both inner and outer pore walls of the CMK-5 models. The functional groups were added in two ways to study the effect of concentration and location of functional groups on water adsorption: (a) functional groups attached in 2 cylindrical shells and (b) functional groups attached in 4 cylindrical shells. It was found that the adsorption phenomena start at lower chemical potential in the carbon models with functional groups, where the water molecules are adsorbed forming small clusters. On increasing chemical potential, these adsorbed water molecules act as nuclei for other water molecules to adsorb via hydrogen bonding, resulting in the growth of clusters. The clusters grow near each cylindrical shell of the functional groups and finally merge to completely fill the pore. The shapes of the computed adsorption isotherms in the CMK models with functional groups are similar to the experimental findings. However, the models without functional groups show a steeped isotherm with a drastic increase of the adsorption amount at certain chemical potentials. In addition to the adsorption isotherms, the results of the computed isosteric heat of adsorption as a function of the adsorbed amount are in good agreement with the experimental results. On the other hand, the models without functional groups fail in reproducing the experimental observations, in particular in the low coverage regime where the host−guest interactions are more important.

The analysis of the hydrogen bond statistics of confined water shows slight variations with the behavior in the bulk. The fraction of water molecules with 3 and 4 hydrogen bonds is larger in pores as compared to the bulk. This confirms that the water molecules confined in the pore walls exhibit a stronger hydrogen bond network than that found in the bulk. We also found different behaviors in the hydrogen bonds of water molecules in the inner and outer porosities of the CMK-5 model.

The cluster size distributions for all the three CMK models show that water molecules form small clusters around functional groups at low chemical potential, and these clusters grow, merge, and result in complete pore filling at higher chemical potential. For all the CMK models with 4 cylindrical shells, there are 4 water clusters observed, and 2 water clusters were observed for CMK models with 2 cylindrical shells at lower chemical potential. It was found that the pore filling occurs at lower chemical potential for all the CMK models with 4 cylindrical shells as compared to CMK models with 2 cylindrical shells.

The effect of the addition of functional groups is also remarkable in the diffusion of water in the three CMK carbon models. In concordance with the stronger host−guest interactions found in the energetic analysis, the presence of functional groups lowers the self-diffusion of water molecules about two magnitude orders compared to the models without functional groups. The consequences of the lower mobility of the water molecules in CMK models with functional groups is also evidenced in the average occupation profiles of the molecules during the MD simulations.

The results from this work highlight the importance of the addition of functional groups in the pores of the CMK-1, CMK-3, and CMK-5 carbon models in order to describe properly the adsorption of water in these hydrophobic mesoporous materials.

■ ASSOCIATED CONTENT

Supporting Information

The Supporting Information is available free of charge on the ACS Publications website at DOI: 10.1021/acsanm.9b01633.

Pore size distributions, experimental adsorption isotherms, additional snapshots of water adsorption in the various models, pair correlation function, self-diffusion coefficients of water in the various models, potential parameters, average numbers of molecules and energies with their corresponding errors, tables minimum and maximum distances, and cluster statistics (PDF)

■ AUTHOR INFORMATION

Corresponding Author

*E-mail: pengxuan@mail.buct.edu.cn (X.P.).

ORCID

Xuan Peng: 0000-0003-3220-7957

Jose Manuel Vicent-Luna: 0000-0001-8712-5591

Jayant Kumar Singh: 0000-0001-8056-2115

Notes

The authors declare no competing financial interest.

■ ACKNOWLEDGMENTS

This research work is supported by the National Natural Science Foundation of China (No. 21676006) and the "CHEMCLOUDCOMPUTING" project. We thank C3UPO for the HPC support.

■ REFERENCES

(1) Jiang, S.; Rhykerd, C. L.; Gubbins, K. E. Layering, Freezing Transitions, Capillary Condensation and Diffusion of Methane in Slit Carbon Pores. *Mol. Phys.* **1993**, *79* (2), 373−391.

(2) Cracknell, R. F.; Nicholson, D.; Quirke, N. A Grand Canonical Monte Carlo Study of Lennard-Jones Mixtures in Slit Shaped Pores. *Mol. Phys.* **1993**, *80* (4), 885−897.

(3) Gregg, S. J. S.; Sing, K. S. W. *Adsorption, Surface Area and Porosity*, 2nd ed.; Academic Press: London, 1982.

(4) Nguyen, T. X.; Bhatia, S. K. How Water Adsorbs in Hydrophobic Nanospaces. *J. Phys. Chem. C* **2011**, *115* (33), 16606−16612.

(5) Nguyen, T. X.; Bhatia, S. K. Some Anomalies in the Self-Diffusion of Water in Disordered Carbons. *J. Phys. Chem. C* **2012**, *116* (5), 3667−3676.

(6) Jorge, M.; Schumacher, C.; Seaton, N. A. Simulation Study of the Effect of the Chemical Heterogeneity of Activated Carbon on Water Adsorption. *Langmuir* **2002**, *18* (24), 9296−9306.

(7) Striolo, A.; Chialvo, A. A.; Cummings, P. T.; Gubbins, K. E. Water Adsorption in Carbon-Slit Nanopores. *Langmuir* **2003**, *19* (20), 8583−8591.

(8) Striolo, A.; Chialvo, A. A.; Cummings, P. T.; Gubbins, K. E. Simulated Water Adsorption in Chemically Heterogeneous Carbon Nanotubes. *J. Chem. Phys.* **2006**, *124* (7), 074710.

(9) Striolo, A.; Chialvo, A. A.; Gubbins, K. E.; Cummings, P. T. Water in Carbon Nanotubes: Adsorption Isotherms and Thermody-

DOI: 10.1021/acsanm.9b01633
ACS Appl. Nano Mater. 2019, 2, 7103−7113

namic Properties from Molecular Simulation. *J. Chem. Phys.* **2005**, *122* (23), 234712.
(10) Birkett, G. R.; Do, D. D. Simulation Study of Water Adsorption on Carbon Black: The Effect of Graphite Water Interaction Strength. *J. Phys. Chem. C* **2007**, *111* (15), 5735−5742.
(11) Picaud, S.; Collignon, B.; Hoang, P. N. M.; Rayez, J.-C. Adsorption of Water Molecules on Partially Oxidized Graphite Surfaces: A Molecular Dynamics Study of the Competition between OH and COOH Sites. *Phys. Chem. Chem. Phys.* **2008**, *10* (46), 6998−7009.
(12) Ohba, T.; Kaneko, K. Surface Oxygen-Dependent Water Cluster Growth in Carbon Nanospaces with GCMC Simulation-Aided in Situ SAXS. *J. Phys. Chem. C* **2007**, *111* (17), 6207−6214.
(13) Ohba, T.; Kaneko, K. Cluster-Associated Filling of Water Molecules in Slit-Shaped Graphitic Nanopores. *Mol. Phys.* **2007**, *105* (2−3), 139−145.
(14) Liu, J.-C.; Monson, P. A. Does Water Condense in Carbon Pores? *Langmuir* **2005**, *21* (22), 10219−10225.
(15) Wongkoblap, A.; Do, D. D. The Effects of Curvature and Surface Heterogeneity on the Adsorption of Water in Finite Length Carbon Nanopores: A Computer Simulation Study. *Mol. Phys.* **2008**, *106* (5), 627−641.
(16) Wongkoblap, A.; Do, D. D. Adsorption of Polar and Nonpolor Fluids in Finite-Length Carbon Slit Pore: A Monte Carlo Simulation Study. *Chem. Eng. Commun.* **2008**, *195* (11), 1382−1395.
(17) Nguyen, V. T.; Horikawa, T.; Do, D. D.; Nicholson, D. Water as a Potential Molecular Probe for Functional Groups on Carbon Surfaces. *Carbon* **2014**, *67*, 72−78.
(18) Zeng, Y.; Prasetyo, L.; Nguyen, V. T.; Horikawa, T.; Do, D. D.; Nicholson, D. Characterization of Oxygen Functional Groups on Carbon Surfaces with Water and Methanol Adsorption. *Carbon* **2015**, *81*, 447−457.
(19) Klomkliang, N.; Kaewmanee, R.; Saimoey, S.; Intarayothya, S.; Do, D. D.; Nicholson, D. Adsorption of Water and Methanol on Highly Graphitized Thermal Carbon Black: The Effects of Functional Group and Temperature on the Isosteric Heat at Low Loadings. *Carbon* **2016**, *99*, 361−369.
(20) Liu, L.; Tan, S.; Horikawa, T.; Do, D. D.; Nicholson, D.; Liu, J. Water Adsorption on Carbon - A Review. *Adv. Colloid Interface Sci.* **2017**, *250*, 64−78.
(21) Canivet, J.; Fateeva, A.; Guo, Y.; Coasne, B.; Farrusseng, D. Water Adsorption in MOFs: Fundamentals and Applications. *Chem. Soc. Rev.* **2014**, *43* (16), 5594−5617.
(22) Zhou, L.; Sun, Y.; Zhou, Y. Enhancement of the Methane Storage on Activated Carbon by Preadsorbed Water. *AIChE J.* **2002**, *48* (10), 2412−2416.
(23) Yazaydın, A. Ö.; Benin, A. I.; Faheem, S. A.; Jakubczak, P.; Low, J. J.; Willis, R. R.; Snurr, R. Q. Enhanced CO2 Adsorption in Metal-Organic Frameworks via Occupation of Open-Metal Sites by Coordinated Water Molecules. *Chem. Mater.* **2009**, *21* (8), 1425−1430.
(24) Müller, E. A.; Rull, L. F.; Vega, L. F.; Gubbins, K. E. Adsorption of Water on Activated Carbons: A Molecular Simulation Study. *J. Phys. Chem.* **1996**, *100* (4), 1189−1196.
(25) McCallum, C. L.; Bandosz, T. J.; McGrother, S. C.; Müller, E. A.; Gubbins, K. E. A Molecular Model for Adsorption of Water on Activated Carbon: Comparison of Simulation and Experiment. *Langmuir* **1999**, *15* (2), 533−544.
(26) Brennan, J. K.; Bandosz, T. J.; Thomson, K. T.; Gubbins, K. E. Water in Porous Carbons. *Colloids Surf., A* **2001**, *187*−*188*, 539−568.
(27) Brennan, J. K.; Thomson, K. T.; Gubbins, K. E. Adsorption of Water in Activated Carbons: Effects of Pore Blocking and Connectivity. *Langmuir* **2002**, *18* (14), 5438−5447.
(28) Wongkoblap, A.; Do, D. D. Adsorption of Water in Finite Length Carbon Slit Pore: Comparison between Computer Simulation and Experiment. *J. Phys. Chem. B* **2007**, *111* (50), 13949−13956.
(29) Mahle, J. J.; Friday, D. K. Water Adsorption Equilibria on Microporous Carbons Correlated Using a Modification to the Sircar Isotherm. *Carbon* **1989**, *27* (6), 835−843.
(30) Kimura, T.; Kanoh, H.; Kanda, T.; Ohkubo, T.; Hattori, Y.; Higaonna, Y.; Denoyel, R.; Kaneko, K. Cluster-Associated Filling of Water in Hydrophobic Carbon Micropores. *J. Phys. Chem. B* **2004**, *108* (37), 14043−14048.
(31) Ohba, T.; Kanoh, H.; Kaneko, K. Cluster-Growth-Induced Water Adsorption in Hydrophobic Carbon Nanopores. *J. Phys. Chem. B* **2004**, *108* (39), 14964−14969.
(32) Vartapetyan, R. S.; Voloshchuk, A. M.; Buryak, A. K.; Artamonova, C. D.; Belford, R. L.; Ceroke, P. J.; Kholine, D. V.; Clarkson, R. B.; Odintsov, B. M. Water Vapor Adsorption on Chars and Active Carbons−Oxygen Sensors Prepared from a Tropical Tree Wood. *Carbon* **2005**, *43* (10), 2152−2159.
(33) Birkett, G. R.; Do, D. D. The Adsorption of Water in Finite Carbon Pores. *Mol. Phys.* **2006**, *104* (4), 623−637.
(34) Picaud, S.; Hoang, P. N. M.; Hamad, S.; Mejias, J. A.; Lago, S. Theoretical Study of the Adsorption of Water on a Model Soot Surface: II. Molecular Dynamics Simulations. *J. Phys. Chem. B* **2004**, *108* (17), 5410−5415.
(35) Morimoto, T.; Miura, K. Adsorption Sites for Water on Graphite. 2. Effect of Autoclave Treatment of Sample. *Langmuir* **1986**, *2* (1), 43−46.
(36) Miura, K.; Morimoto, T. Adsorption Sites for Water on Graphite. 3. Effect of Oxidation Treatment of Sample. *Langmuir* **1986**, *2* (6), 824−828.
(37) Miura, K.; Morimoto, T. Adsorption Sites for Water on Graphite. 5. Effect of Hydrogen-Treatment of Graphite. *Langmuir* **1991**, *7* (2), 374−379.
(38) Miura, K.; Morimoto, T. Adsorption Sites for Water on Graphite. 6. Effect of Ozone Treatment of Sample. *Langmuir* **1994**, *10* (3), 807−811.
(39) Sarkisov, L.; Centineo, A.; Brandani, S. Molecular Simulation and Experiments of Water Adsorption in a High Surface Area Activated Carbon: Hysteresis, Scanning Curves and Spatial Organization of Water Clusters. *Carbon* **2017**, *118*, 127−138.
(40) Thommes, M.; Morell, J.; Cychosz, K. A.; Fröba, M. Combining Nitrogen, Argon, and Water Adsorption for Advanced Characterization of Ordered Mesoporous Carbons (CMKs) and Periodic Mesoporous Organosilicas (PMOs). *Langmuir* **2013**, *29* (48), 14893−14902.
(41) Weinberger, C.; Cao, X.; Tiemann, M. Selective Surface Modification in Bimodal Mesoporous CMK-5 Carbon. *J. Mater. Chem. A* **2016**, *4* (47), 18426−18431.
(42) Jain, S. K.; Pellenq, R. J.-M.; Gubbins, K. E.; Peng, X. Molecular Modeling and Adsorption Properties of Ordered Silica-Templated CMK Mesoporous Carbons. *Langmuir* **2017**, *33* (9), 2109−2121.
(43) Peng, X.; Jain, S. K.; Singh, J. K.; Liu, A.; Jin, Q. Formation Patterns of Water Clusters in CMK-3 and CMK-5 Mesoporous Carbons: A Computational Recognition Study. *Phys. Chem. Chem. Phys.* **2018**, *20* (25), 17093−17104.
(44) Peng, X.; Jain, S. K. Understanding the Influence of Pore Heterogeneity on Water Adsorption in Realistic Molecular Models of Activated Carbons. *J. Phys. Chem. C* **2018**, *122* (50), 28702−28711.
(45) Moulin, F.; Picaud, S.; Hoang, P. N. M.; Jedlovszky, P. Grand Canonical Monte Carlo Simulation of the Adsorption Isotherms of Water Molecules on Model Soot Particles. *J. Chem. Phys.* **2007**, *127* (16), 164719.
(46) Peng, X.; Jain, S. K.; Singh, J. K. Adsorption and Separation of N2/CH4/CO2/SO2 Gases in Disordered Carbons Obtained Using Hybrid Reverse Monte Carlo Simulations. *J. Phys. Chem. C* **2017**, *121* (25), 13457−13473.
(47) Peng, X.; Lin, L.; Sun, W.; Smit, B. Water Adsorption in Metal-Organic Frameworks with Open-Metal Sites. *AIChE J.* **2015**, *61* (2), 677−687.
(48) Swiatla-Wojcik, D. Evaluation of the Criteria of Hydrogen Bonding in Highly Associated Liquids. *Chem. Phys.* **2007**, *342* (1), 260−266.
(49) Bhattacharya, S.; Gubbins, K. E. Fast Method for Computing Pore Size Distributions of Model Materials. *Langmuir* **2006**, *22* (18), 7726−7731.

DOI: 10.1021/acsanm.9b01633
ACS Appl. Nano Mater. 2019, 2, 7103−7113

(50) Aristov, Y. I. Adsorptive Transformation of Heat: Principles of Construction of Adsorbents Database. *Appl. Therm. Eng.* **2012**, *42*, 18−24.
(51) Lehmann, C.; Beckert, S.; Gläser, R.; Kolditz, O.; Nagel, T. Assessment of Adsorbate Density Models for Numerical Simulations of Zeolite-Based Heat Storage Applications. *Appl. Energy* **2017**, *185*, 1965−1970.

DOI: 10.1021/acsanm.9b01633
ACS Appl. Nano Mater. 2019, 2, 7103−7113